CAMBRIDGE
UNIVERSITY PRESS

Article

Bowlesite, PtSnS, a new platinum group mineral (PGM) from the Merensky Reef of the Bushveld Complex, South Africa

Anna Vymazalová[1]* ⓘ, Federica Zaccarini[2], Giorgio Garuti[2], František Laufek[1], Daniela Mauro[3], Chris J. Stanley[4] and Cristian Biagioni[3]

[1]Czech Geological Survey, Geologická 6, 152 00, Praha 5, Czech Republic; [2]Department of Applied Geological Sciences and Geophysics, University of Leoben, Peter Tunner Str. 5, A-8700 Leoben, Austria; [3]Dipartimento di Scienze della Terra, Università di Pisa, Via Santa Maria 53, I-56126 Pisa, Italy; and [4]Department of Earth Sciences, Natural History Museum, London SW7 5BD, United Kingdom

Abstract

Bowlesite is a new mineral discovered in the Merensky Reef of the Rustenburg Platinum Mine, Bushveld complex, South Africa. Bowlesite forms tiny grains (maximum dimension 20 µm). It is associated with sulfides including chalcopyrite, pyrrhotite and pentlandite, in contact with silicates including plagioclase, pyroxene- and minor serpentine-subgroup and amphibole-supergroup minerals. Bowlesite is brittle and has a metallic lustre. In plane-polarised light, bowlesite has a light bluish grey colour. It shows weak bireflectance, no pleochroism and has weak anisotropism. Internal reflections were not observed. Reflectance values of bowlesite in air (R_1, R_2 in %) are: 50.3–51.4 at 470 nm, 48.5–48.9 at 546 nm, 47.9–48.6 at 589 nm and 47.8–48.7 at 650 nm. Ten spot analyses of bowlesite give the average composition: Pt 56.85, Pd 0.02, Sn 34.03 and S 9.15, total 100.05 wt.%, corresponding to the empirical formula $(Pt_{1.001}Pd_{0.001})_{\Sigma1.002}Sn_{0.997}S_{1.001}$, based on 3 atoms per formula unit. The simplified formula is PtSnS. Due to the small size of bowlesite, the crystal structure was solved and refined from the powder X-ray-diffraction data of synthetic PtSnS. The calculated density is 10.06 g·cm⁻³. The mineral is orthorhombic, space group: $Pca2_1$ (#29) with $a = 6.11511(10)$, $b = 6.12383(10)$, $c = 6.09667(11)$ Å, $V = 228.31(1)$ Å₃ and $Z = 4$. Bowlesite is isotypic with cobaltite, CoAsS. The origin of bowlesite is probably related to low-T exsolution of Pt–Sn phases from high-T sulfides crystallised from the sulfide melt. The mineral honours Dr. John Bowles (Manchester University, UK) for his contributions to ore mineralogy and mineral deposits related to mafic–ultramafic rocks.

Keywords: bowlesite, platinum-group mineral, PtSnS, crystal structure, Merensky Reef, Bushveld complex, South Africa

Introduction

The Merensky Reef consists of a horizon of medium to coarse-grained cumulate feldspathic pyroxenites, anorthosite and chromitite along with interstitial sulfides (Barnes and Maier, 2002). There is a wide range of platinum-group minerals (PGM) occurring in the Merensky Reef (e.g. Brynard *et al.*, 1976; Vermaak and Hendriks, 1976; Kinloch, 1982; Oberthür *et al.*, 2004, 2016) and it is a type or co-type locality for PGM like cooperite, braggite, merenskyite, atokite and rustenburgite (Wagner, 1929; Bannister and Hey, 1932; Kingston, 1966; Mihálik *et al.*, 1975).

During the examination of a sample collected by one of the authors (G.G.) during the third International Platinum Symposium held in Pretoria (South Africa) from 6 to 10 July 1981 (Vermaak and Von Gruenewaldt, 1981), a PGM with the chemical composition PtSnS was detected. A mineral with this composition does not correspond to any valid or invalid unnamed mineral listed in Smith and Nickel (2007).

A mineral with the same chemical composition as bowlesite was first mentioned by Cousins and Kinloch (1976) from the Merensky Reef, Bushveld complex, and later by Kinloch (1982) from the Platreef of the Bushveld complex, by Barkov *et al.* (2001), Osbahr (2012) and Osbahr *et al.* (2013) from the Merensky Reef. In addition, a PtSnS compound was described from the Hartley platinum mine of the Great Dyke in Zimbabwe (Oberthür *et al.*, 2003).

Both the mineral and its name were approved by the Commission on New Minerals, Nomenclature and Classification of the International Mineralogical Association, under the number IMA 2019-079 (Vymazalová *et al.*, 2019). The mineral is named to honour John Frederick William Bowles (b. 1941), honorary visitor at Manchester University, UK, for his contributions to ore mineralogy and mineral deposits related to mafic–ultramafic rocks.

Holotype material (polished section), along with its synthetic analogue (experiment number Pt13_600), is deposited at the Department of Earth Sciences of the Natural History Museum, London, UK, catalogue number BM 2019,11. Anthropotype material is also kept in the mineralogical collection of the

*Author for correspondence: Anna Vymazalová, Email: anna.vymazalova@geology.cz
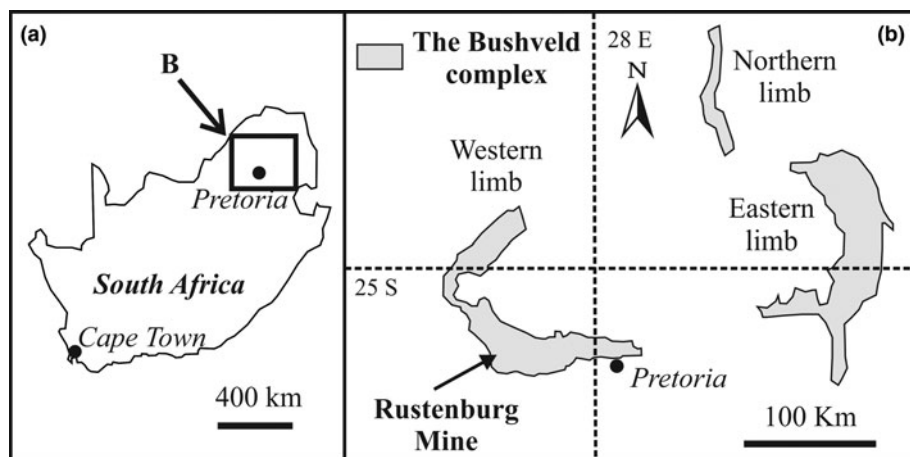
Museo di Storia Naturale, Università di Pisa, Italy, under the catalogue number 19909.

Occurrence

Bowlesite was found in the Merensky Reef of the Bushveld layered intrusion of South Africa. The Bushveld complex occurs north of Pretoria (Fig. 1*a*) and is divided into three major limbs: eastern, western and northern (Fig. 1*b*). The studied sample was collected underground in the Rustenburg mine (Rustenburg Section) by one of the authors (G.G.). Rustenburg platinum mine (25°32′S, 27°11′E) is located in the western limb of the Bushveld complex, ~100 km west of Pretoria (Fig. 1).

Bowlesite was discovered in two square polished blocks (each *ca*. 2.5 cm × 2.5 cm), representing a portion of the typical Merensky reef exposed in the Rustenburg Section. It consists of a mineralised layer ~0.30 m thick between two thin chromitite layers, marking the top and the bottom contacts of the reef (Vermaak and Von Gruenewaldt, 1981).

Confirming the petrographic description provided by Ballhaus and Stumpfl (1986) and Nicholson and Mathez (1991), the studied polished blocks comprise a thin layer of cumulitic chromitite, ~0.2 cm thick, in contact with a pegmatoidal feldspathic pyroxenite that contains accessory actinolite, micas, talc, chlorite and a serpentine-subgroup mineral. The plagioclase shows a composition corresponding to 'andesine', while the pyroxenes can be classified as augite and enstatite.

The investigated polished blocks contain up to 25% interstitial sulfides, mainly pyrrhotite, pentlandite and chalcopyrite. A reflected-light microphotograph showing chromite, silicates and sulfides occurring in the holotype material is presented in Fig. 2.

Bowlesite is hosted within sulfides only and it occurs in contact with the interstitial silicates, mainly represented by plagioclase, pyroxene, minor serpentine-subgroup and amphibole-supergroup minerals and rare calcite (Fig. 3). In the sample studied bowlesite was never found included in chromite, but is associated typically with chalcopyrite; the association with pyrrhotite is rarer. It was also observed in contact with moncheite (Fig. 3).

Appearance, and physical and optical properties

In polished sections, bowlesite occurs as anhedral to subhedral tiny grains (from a few μm up to ~20 μm), associated with chalcopyrite, pyrrhotite and pentlandite. It occurs in contact with the interstitial silicates, mainly plagioclase, pyroxene and minor serpentine-subgroup and amphibole-supergroup minerals (Fig. 3).

Bowlesite is brittle and has a metallic lustre. In plane-polarised light, in association with chalcopyrite, pyrrhotite, pentlandite and moncheite, bowlesite has a pale bluish grey colour. It is very weakly bireflectant and has no pleochroism. It has a very weak anisotropism with indeterminate rotation tints. Internal reflections were not observed.

The reflectance measurements on bowlesite and its synthetic equivalent were carried-out using a WTiC standard and a J&M TIDAS diode array spectrophotometer at the Natural History Museum in London, UK. Reflectance values of bowlesite and its synthetic analogue in air (R_1, R_2 in %) are listed in Table 1 and illustrated in Fig. 4.

Density was not measured because of the small amount of available material and the presence of fine intergrowths with moncheite. The calculated density is 10.06 g.cm^{-3}, based on the empirical composition and unit-cell volume refined from powder X-ray diffraction data of the synthetic analogue.

Synthetic analogue

The small size of available grains of bowlesite prevented its extraction and isolation in an amount sufficient for the relevant
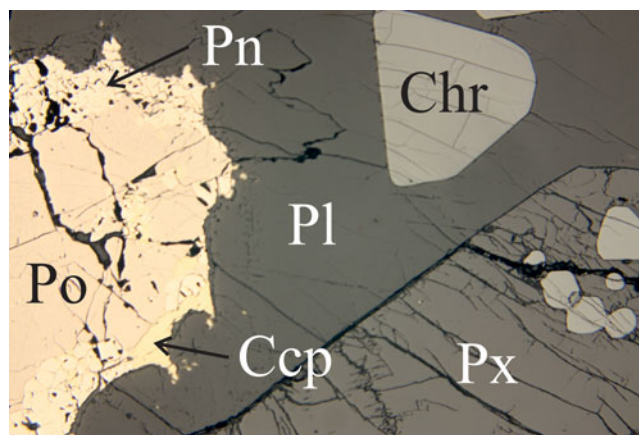

Fig. 2. Reflected-light microphotograph of the studied sample containing bowlesite. Abbreviations: Po = pyrrhotite, Pn = pentlandite, Ccp = chalcopyrite, Chr = chromite, Pl = plagioclase, Px = pyroxene. Field of view: 4 mm, sample no. MR 4.
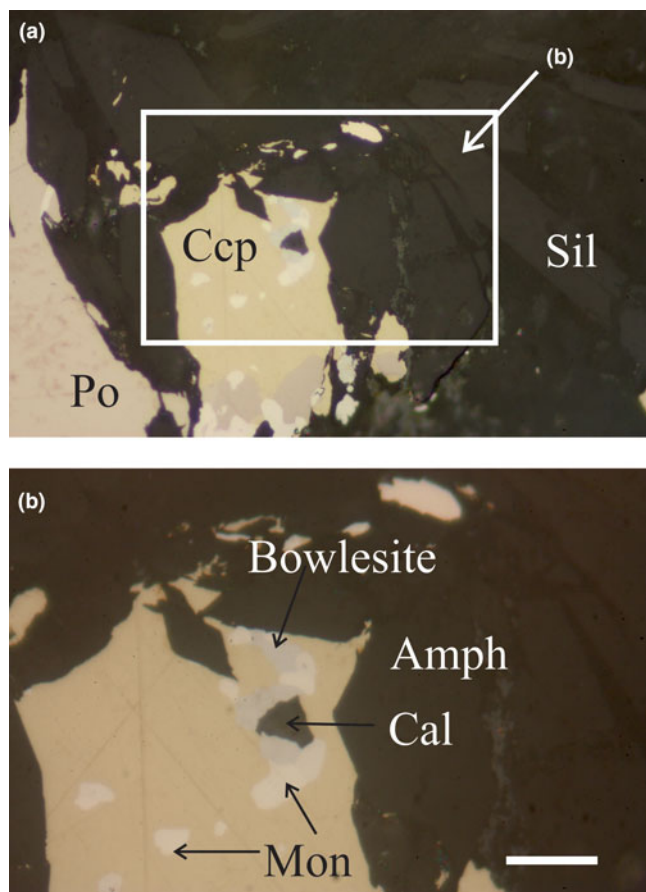
Fig. 3. (*a*) Reflected-light microphotograph showing the mineralogical assemblage in which bowlesite occurs. (*b*) Enlargement of (*a*). Abbreviations: Ccp = chalcopyrite, Amph = amphibole, Cal = calcite and Mon = moncheite. Scale bar is 20 μm., sample no. MR 4
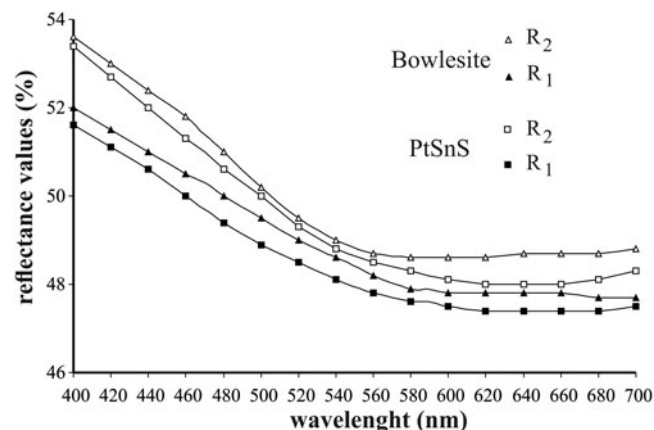

Fig. 4. Reflectance data of bowlesite and its synthetic analogue PtSnS in air. Reflectance values (*R*%) are plotted versus wavelength (λ, in nm).

crystallographic and structural investigations. Therefore, these investigations were performed on its synthetic analogue.

Synthetic PtSnS was prepared using the evacuated silica glass tube method in the Laboratory of Experimental Mineralogy of the Czech Geological Survey in Prague. Platinum (99.95%), tin (99.9999%) and sulfur (99.9999%) were used as starting materials for the synthesis. The evacuated tube with its charge was sealed, heated at 300°C for 1 month and afterwards annealed at 1000°C for 2 days. After cooling in a cold-water bath, the charge was ground to powder in acetone using an agate mortar, and mixed thoroughly to homogenise. The pulverised charge was sealed in an evacuated silica-glass tube again, and re-heated at 600°C for 7 months. The experimental product was quenched rapidly in cold water. The experimental product was first investigated by a field emission scanning electron microscope and by means of the powder X-ray diffraction analyses.

Chemical composition

Quantitative chemical analyses and acquisition of back-scattered electron images of bowlesite were performed with a JEOL JXA-8200 electron-microprobe, installed in the E. F. Stumpfl laboratory, Leoben University, Austria, operating in WDS (wavelength dispersive spectrometry) mode. Major and minor elements were determined at 20 kV accelerating voltage and 10 nA beam current, with 20 s as the counting time for the peaks and 10 s for the backgrounds. The beam diameter was ~1 μm in size. The *K*α line was used for S and *L*α for Pt, Pd and Sn. The following diffracting crystals were selected: PETJ for S, LIFH for Pt and PETH for Pd and Sn. Synthetic standards were: PtSn for Pt and Sn; PtS for S; and metallic palladium for Pd. The ZAF correction method was applied.

In order to verify the homogeneity and composition, the synthetic analogue of bowlesite was analysed using a CAMECA SX-100 electron probe microanalyser in WDS mode, at the Geological Institute of the Czech Academy of Sciences, Czech Republic. Pure elements and marcasite were used as standards and the spectral lines measured were *K*α for S, *L*α for Sn, and *M*α for Pt, with an accelerating voltage of 15 kV, and a beam current of 10 nA measured on the Faraday cup.

Quantitative chemical analysis (Table 2) proved that bowlesite is characterised by the empirical formula $(Pt_{1.001}Pd_{0.001})_{\Sigma1.002}$ $Sn_{0.997}S_{1.001}$, based on 3 atoms per formula unit and by the ideal

Table 1. Reflectance values for bowlesite and the synthetic PtSnS in air.

	Bowlesite		PtSnS	
λ/nm	R_1 (%)	R_2 (%)	R_1 (%)	R_2 (%)
400	52.0	53.6	51.6	53.4
420	51.5	53.0	51.1	52.7
440	51.0	52.4	50.6	52.0
460	50.5	51.8	50.0	51.3
470	**50.3**	**51.4**	**49.7**	**51.0**
480	50.0	51.0	49.4	50.6
500	49.5	50.2	48.9	50.0
520	49.0	49.5	48.5	49.3
540	48.6	49.0	48.1	48.8
546	**48.5**	**48.9**	**48.0**	**48.7**
560	48.2	48.7	47.8	48.5
580	47.9	48.6	47.6	48.3
589	**47.9**	**48.6**	**47.6**	**48.2**
600	47.8	48.6	47.5	48.1
620	47.8	48.6	47.4	48.0
640	47.8	48.7	47.4	48.0
650	**47.8**	**48.7**	**47.4**	**48.0**
660	47.8	48.7	47.4	48.0
680	47.7	48.7	47.4	48.1
700	47.7	48.8	47.5	48.3

The values required by the Commission on Ore Mineralogy are given in bold.

Table 2. Chemical composition (in wt.%) for bowlesite and the synthetic PtSnS.

Constituent	Pt	Pd	Sn	S	Total
Bowlesite (n = 10)					
Average	56.85	0.02	34.03	9.15	100.05
Range	53.97–57.59	0.00–0.10	33.73–34.82	8.93–9.77	98.21–101.50
S.D.	1.11	0.46	0.04	0.24	0.98
Synthetic equivalent (n = 12)					
Average	55.47		35.23	9.43	100.13
Range	54.69–56.16		34.97–35.51	9.26–9.59	99.34–100.95
S.D.	0.41		0.17	0.11	0.44
Ideal composition					
	56.41		34.32	9.27	100

S.D. – standard deviation

Table 3. Powder diffraction data collection and Rietveld analysis of the synthetic analogue of bowlesite, PtSnS.

Crystal data	
Formula	PtSnS
Space group	$Pca2_1$ (29)
Unit-cell content	PtSnS, $Z = 4$
Unit-cell parameters (Å)	$a = 6.11511(10)$
	$b = 6.12383(10)$
	$c = 6.09667(11)$
Unit-cell volume (Å^3)	228.31(1)
Data collection	
Radiation type, source	X-ray, Cu$K\alpha$
Generator settings	40 kV, 30 mA
Range in 2θ (°)	10–140
Step size (°)	0.007
Rietveld analysis	
No. of reflections	241
No. of structural parameters	14
No. of profile parameters	2
R_{Bragg}	0.074
R_p	0.068
R_{wp}	0.089
Weighting scheme	$1/y_o$

and simplified formula PtSnS corresponding to (in wt.%) Pt 56.41, Sn 34.32, S 9.27, total 100.00. This composition fits perfectly with those of the synthetic $Pt_{0.97}Sn_{1.02}S_{0.95}$: Pt 55.47, Sn 35.23 and S 9.43 (wt.%), Table 2.

X-ray crystallography

Crystal structure investigations were performed on synthetic PtSnS only. Powder X-ray diffraction data were collected in Bragg-Brentano geometry using a Bruker D8 Advance powder diffractometer. Nickel-filtered Cu$K\alpha$ radiation was used, as well as 10 mm automatic divergence slit and a Lynx Eye-XE detector. Data were collected in the angular range from 10 to 140° of 2θ with 0.007° steps. The details of data collection and basic crystallographic data are given in Table 3.

Weihrich *et al.* (2004) performed density functional theory (DFT) calculations of synthetic PtSnS and mentioned that this phase belongs to the pyrite structural family (FeS$_2$, $Pa\bar{3}$), which is characterised by octahedral coordination of transitional metals and S–S bonds, in a 'dumbbell' configuration. Other well-known members of this structural-type family are the minerals ullmannite (NiSbS, $P2_13$) and cobaltite (CoAsS, $Pca2_1$) (Weihrich *et al.*, 2004; Bachhuber *et al.*, 2015; Bayliss, 1989). Weihrich *et al.* (2004) reported another related structure with $R3$ symmetry. A lowering of symmetry from $Pa\bar{3}$ (pyrite-type structure) to $P2_13$ (ullmannite-type structure), to $Pca2_1$ (cobaltite-type structure) or $R3$ structure is achieved through the replacement of homoatomic S–S dumbbells with heteroatomic X–Y pairs (X = Sb, As, Sn, Ge, Pb and Si; Y = S, Se and Te) and related X and Y structural ordering. The three above-mentioned structures (ullmannite, cobaltite-type and $R3$ structure) differ by a distinct ordering scheme of X and Y atoms.

According to the DFT calculation of Weihrich *et al.* (2004), PtSnS should have the $R3$ structure, which is a relatively uncommon structure-type. Although they mentioned small energy differences from DFT calculations between the considered three structural models, no direct crystallographic study was performed by Weihrich *et al.* (2004).

In this work, the four possible structural models for PtSnS have been tested through Rietveld refinement on powder X-ray diffraction data of synthetic PtSnS. Rietveld refinement was performed by means of the *Topas 5* program (Bruker AXS, 2014) and involved refinement of unit-cell parameters, atomic coordinates, isotropic size and strain. Isotropic displacement parameters were fixed during the refinement ($B_{iso} = 0.2$ Å^2 for all atoms). Background was determined by means of a Chebyshev polynomial function of the 5th order. The following structural models have been taken into account: (1) pyrite-type structure ($Pa\bar{3}$):
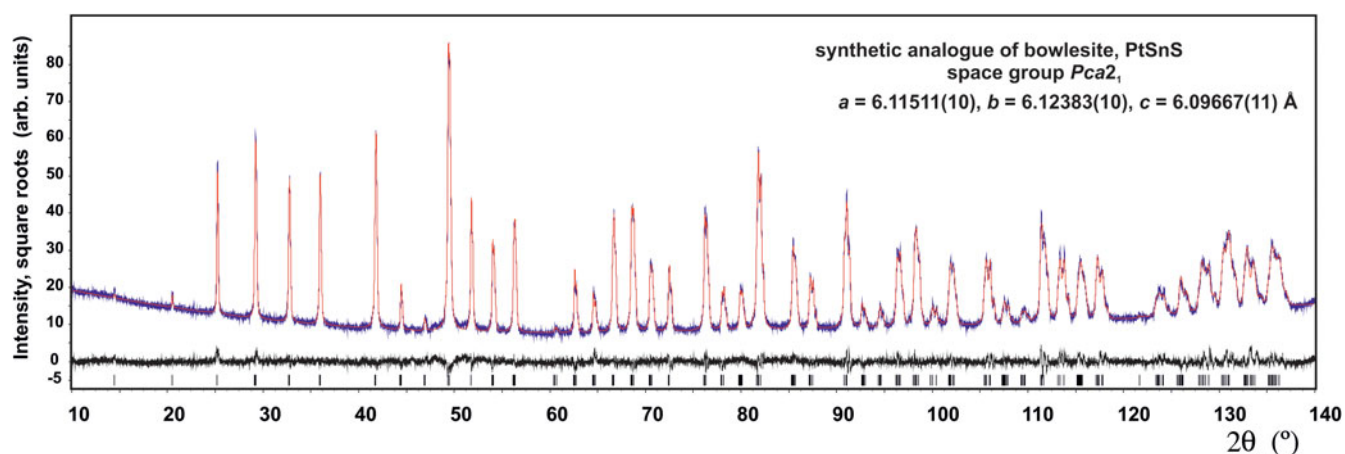
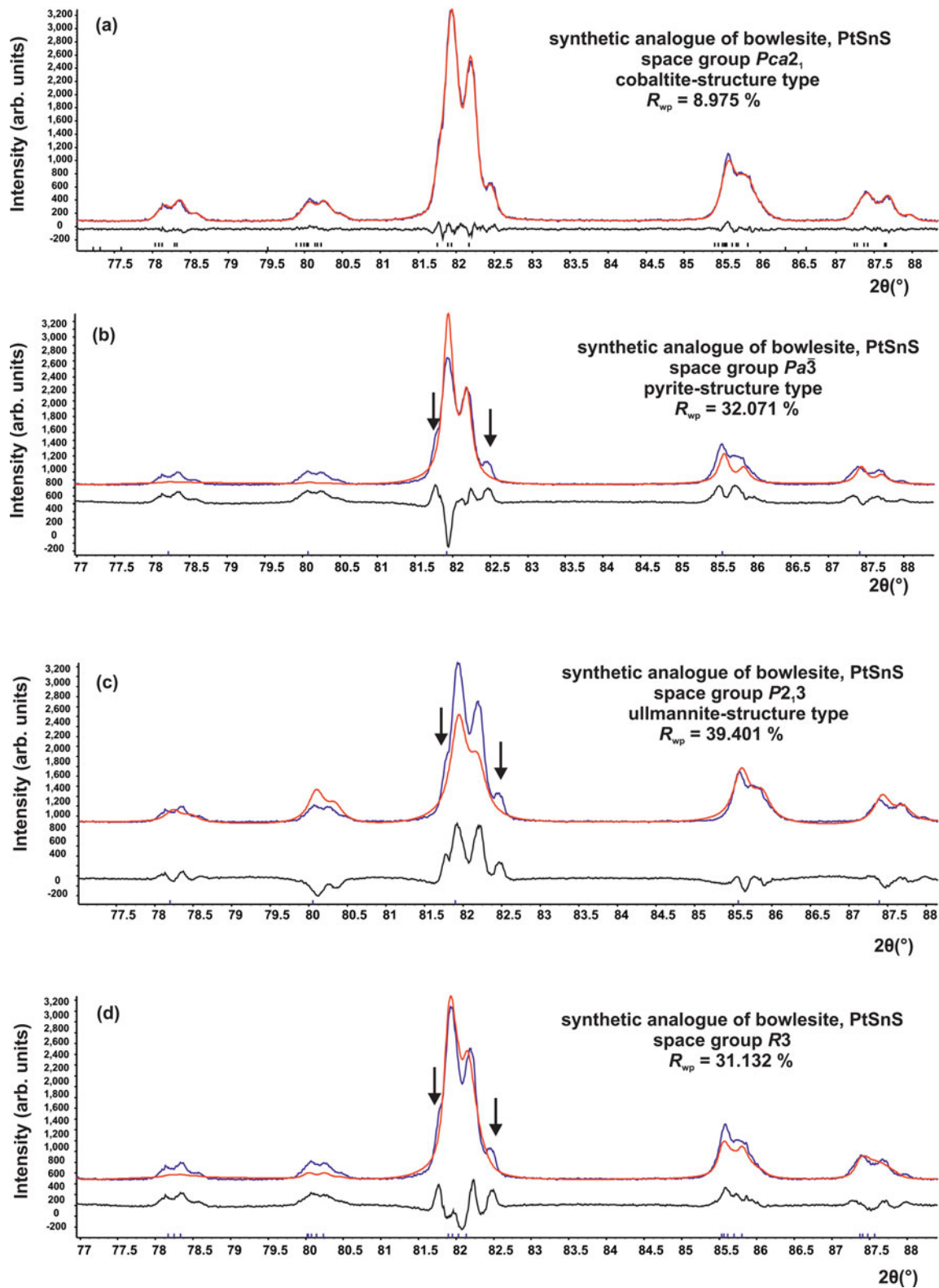**Fig. 5.** The final Rietveld fit for synthetic equivalent of bowlesite, PtSnS.

Fig. 6. Details of the Rietveld refinement of the synthetic analogue of bowlesite, PtSnS, using structure models of (*a*) cobaltite, (*b*) pyrite, (*c*) ullmannite and (*d*) theoretical *R*3 structure. Only the cobaltite-type structure model can fit all observed reflections in the powder X-ray diffraction pattern. The unfitted reflections in other structural models are indicated by arrows. Note the significant difference in R_{wp} agreement factors.

Table 4. Atomic positions (space group *Pca*2₁) for the synthetic analogue of bowlesite, PtSnS.

Atom	Wyckoff letter	x	y	z
Pt	4*a*	0.0092(1)	0.7336(1)	0.0035(3)
Sn	4*a*	0.3817(2)	0.1334(2)	0.6179(3)
S	4*a*	0.6212(6)	0.3752(7)	0.3771(8)

The isotropic displacement parameter B_{iso} was fixed at 0.2 Å for all atoms during the refinement.

Pt at 4*a*; Sn and S disordered at 8*c* positions; (2) ullmannite-type structure (*P*2₁3): Pt, Sn and S at three distinct 4*a* positions; (3) cobaltite-type structure (*Pca*2₁): Pt, Sn and S at three distinct 4*a* positions; and (4) *R*3 structure: Pt at 1*a* and 3*b*, Sn at 1*a* and 3*b*, S at 1*a* and 3*b* distinct positions.

Although the powder X-ray diffraction patterns of phases with pyrite, ullmannite and cobaltite type structures look similar, using diffraction data measured up to a high diffraction angle (145°2θ) and on a diffractometer with a high resolution (e.g. compared to a Gandolfi camera), it is possible to distinguish between all the above-mentioned four structure models. Rietveld refinement (Fig. 5) shows unambiguously that PtSnS adopts the cobaltite structure type (*Pca*2₁). The cubic models with pyrite- and ullmannite-type structures cannot fit either the observed reflections in the powder pattern of PtSnS or the apparent peak splitting. This indicates unambiguously the *Pca*2₁ symmetry. Neither can the structure model proposed by Weihrich *et al.* (2004) in *R*3 space group fit all observed reflections (see Fig. 6). Only the cobaltite-structure model explains all observed reflections, giving a good fit with the split peaks and achieving a significantly lower R_{wp} agreement factor (8.975%) than those for disordered pyrite, ullmannite and *R*3 structure models (32.071, 39.401 and 31.132%, respectively). Therefore, the final refinement of synthetic PtSnS was performed in the *Pca*2₁ symmetry using the cobaltite structure model. Crystal structure and powder-diffraction data are presented in Tables 4 and 5, respectively. The crystallographic information files have been deposited with the Principal Editor of *Mineralogical Magazine* and are available as Supplementary material (see below).
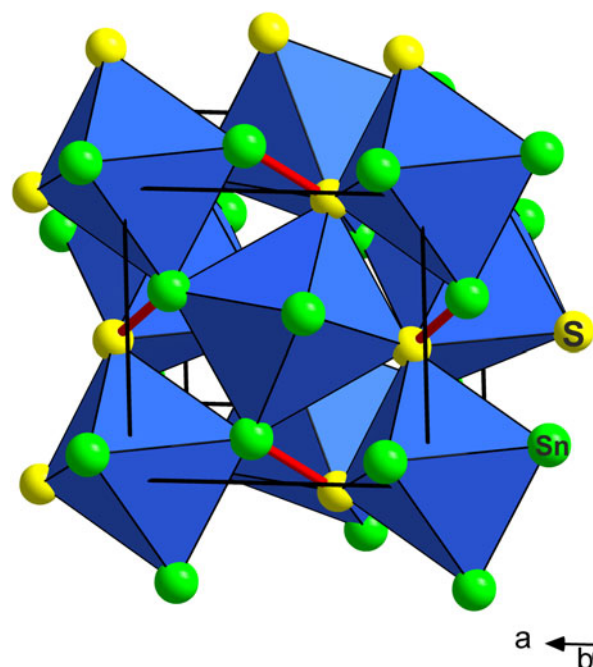
Fig. 7. Crystal structure of synthetic analogue of bowlesite, PtSnS, showing the corner-sharing [PtSn₃S₃] octahedra (in blue). Note the dumbbell configuration, with localised Sn–S bonds (red lines).

Structure description

The crystal structure of bowlesite contains octahedrally coordinated Pt with three S and Sn atoms as ligands. The Sn and S atoms form covalent pairs, with bond distances of 2.548(5) Å. This is slightly longer than the Pt–S distances ranging from 2.459(4) to 2.478(4) Å and at the same time shorter than Pt–Sn distances (2.607(2)–2.632(2) Å). Slightly shorter Pt–S distances were observed in the synthetic analogue of cooperite, PtS (2.312 Å), where Pt shows a square-planar coordination (Groenvold *et al.*, 1960). The structure is formed by corner-sharing [PtSn₃S₃] octahedra (Fig 7). There are three Pt octahedra sharing every anion.

Table 5. X-ray powder diffraction data (d in Å) for PtSnS, the synthetic analogue of bowlesite (Cu$K\alpha$ radiation, Bruker D8 Advance, Bragg-Brentano geometry).

I_{obs}	d_{obs}	d_{calc}	$h\,k\,l$
1	6.1149	6.1237	010
2	4.3264	4.3271	110
21	3.5256	3.5286	111
38	**3.0545**	**3.0619, 3.0575, 3.0483**	**020, 200, 002**
25	**2.7317**	**2.7379, 2.7355, 2.7331, 2.7289**	**120, 210, 201, 012**
26	**2.4948**	**2.4976, 2.4958, 2.4920**	**121, 211, 112**
40	2.1591	2.1636, 2.1603, 2.1587	220, 022, 202
100	**1.8431**	**1.8454, 1.8435, 1.8395**	**131, 311, 113**
19	1.7643	1.7643	222
10	1.6957	1.6977, 1.6968, 1.6961	230, 320, 032
5	1.6926	1.6925	203
18	1.6331	1.6355, 1.6346, 1.6344, 1.6331, 1.6318, 1.6313	231, 321, 132, 312, 123, 213
8	1.4826	1.4833, 1.4832, 1.4829, 1.4826, 1.4813, 1.4790	410, 232, 401, 322, 223, 014
5	1.4424	1.4429, 1.4424	141, 330
23	1.4010	1.4036, 1.4018, 1.4010	331, 133, 313
22	1.3678	1.3689, 1.3681, 1.3678, 1.3666	240, 042, 420, 402
8	1.3643	1.3645, 1.3641	024, 204
10	1.3338	1.3357, 1.3351, 1.3346, 1.3337	241, 142, 421, 412
10	1.3032	1.3038, 1.3029, 1.3025	332, 233, 323
80	**1.2482**	**1.2488, 1.2479, 1.2460**	**242, 422, 224**

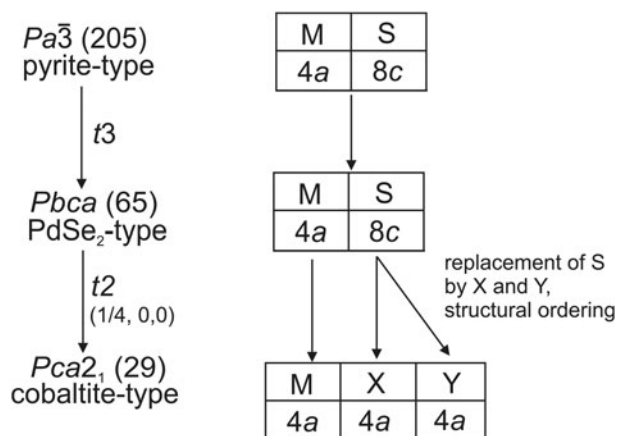The strongest lines are given in bold.

Fig. 8. Symmetry relations for the pyrite-type and the bowlesite crystal structure including splitting of the Wyckoff positions during the reduction of the symmetry. The space group of bowlesite (*Pca2₁*) is a subgroup of the pyrite-type structure (*Pa3̄*).
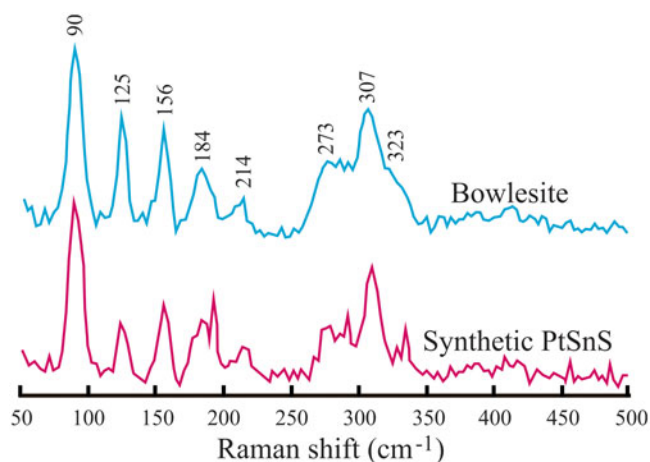

Fig. 9. Raman spectra of bowlesite and its synthetic analogue PtSnS.

The crystal structure of bowlesite is a homeotype of the pyrite structure ($Pa\bar{3}$) and is isotypic with cobaltite. Its structure can be viewed as an ordered ternary variant of the pyrite-type structure with an ordered distribution of Sn and S atoms, replacing the

S–S dumbbells in the pyrite structure. Its derivation from the pyrite-type structure and the corresponding group–subgroup relations are shown in Fig 8. In addition to cobaltite, the most closely related mineral species are milotaite, PdSbSe (Paar *et al.*, 2005) and maslovite, PtBiS (Kovalenker *et al.*, 1979). However, both minerals show cubic symmetry and hence a different ordering scheme of anions.

Bowlesite belongs to the cobaltite group (2.EB.10) of the metal sulfides (M:S ≤ 1:2, 2.E) of the Nickel and Strunz classification.

Verification of identity of bowlesite and its synthetic analogue

The structural identity of bowlesite and its synthetic analogue PtSnS was confirmed by Raman spectroscopy and electron back-scattering diffraction.

Raman Spectroscopy

Micro-Raman spectra were obtained on polished samples in nearly back-scattered geometry with a Jobin-Yvon Horiba XploRA Plus apparatus (Dipartimento di Scienze della Terra, Università di Pisa), equipped with an Olympus BX41 microscope with an 100× objective and a motorised *x-y* stage. The 532 nm line of a solid-state laser was used. The minimum lateral and depth resolution was set to a few µm. The system was calibrated using the 520.6 cm⁻¹ Raman band of silicon before each experimental session.

Raman spectra were collected, in the spectral range between 50 and 1200 cm⁻¹, through multiple acquisitions with single counting times of 60 s. The laser power was filtered at 1%, 10% and 25%, i.e. 0.25, 2.5 and 6.25 mW, respectively. No change was observed on the surface of the samples at the end of the acquisitions and all the collected Raman spectra are in excellent agreement. The backscattered radiation was analysed with a 1200 gr mm⁻¹ grating monochromator.

The Raman spectrum of bowlesite is characterised by bands in the region below 600 cm⁻¹, in agreement with other sulfides (e.g. Mernagh and Trudu, 1993). Figure 9 shows the comparison between bowlesite and its synthetic counterpart. Bowlesite and synthetic PtSnS show the strongest band at 90 cm⁻¹ and several other discernible bands at 125, 156, 184, 214, 273, 307 and 323 cm⁻¹ (Fig. 9).
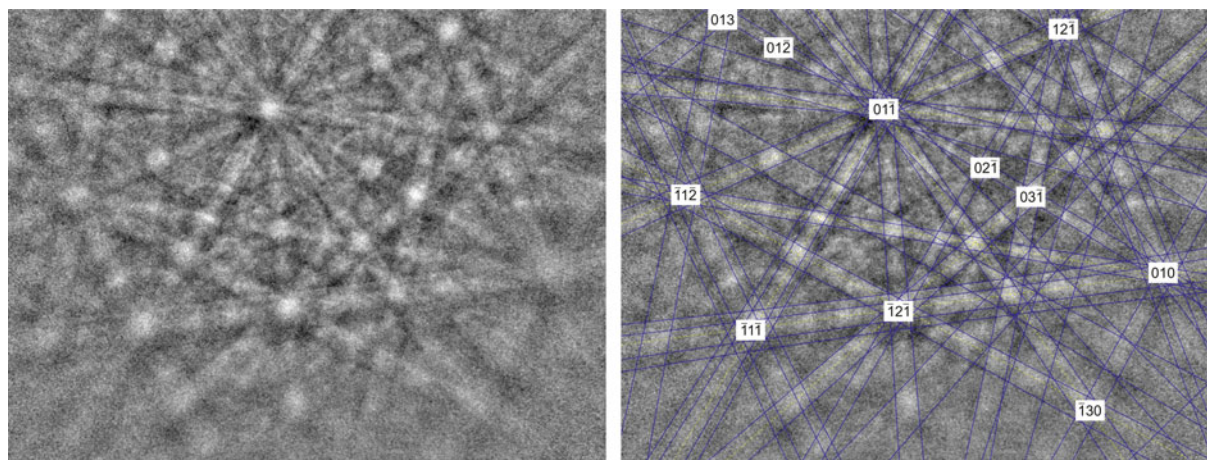

Fig. 10. EBSD image of bowlesite, left: primary EBS patterns; right: the EBS patterns indexed with solution overlain.

Electron back-scattering diffraction

A TESCAN Mira 3GMU scanning electron microscope combined with electron back-scattering diffraction (EBSD) system (NordlysNano detector, Oxford Instruments) available at the Czech Geological Survey, Czech Republic was used for the measurements of the EBSD patterns on bowlesite. The polished section was prepared for investigation by etching the mechanically polished surface with colloidal silica (OP-U, 0.04 µm standard colloidal silica suspension) for 30 minutes to reduce the surface damage. The EBSD patterns were collected and processed using a proprietary computer program AZtec HKL (Oxford Instruments). Kikuchi patterns obtained from the natural material (10 measurements on different spots on bowlesite) were found to match those generated from our refined structural model for PtSnS (Fig. 10). The values of the mean angular deviation (MAD, i.e. goodness of fit of the solution) between the calculated and measured Kikuchi bands range between 0.27° and 0.56°. These values reveal a very good match, as long as values of MAD <1°, they are considered as indicators of an acceptable fit (HKL Technology v. 2004).

Summary and concluding remarks

Bowlesite (PtSnS) is a new PGM discovered in the Merensky Reef, Bushveld complex, South Africa. In the Bushveld Complex, pristine platinum-group element mineralisation is related to sulfide accumulations (between 0.1 and 10 vol.%; mainly pyrrhotite, pentlandite, chalcopyrite and some pyrite), in a manner typical of Ni–Cu-sulfide mineralisation worldwide (Naldrett, 2004).

As a rule, the PGM are associated with the sulfides, commonly intergrown with or sited at sulfide–sulfide or sulfide–silicate grain boundaries, at the peripheries or at contacts of the sulfide grains. Bowlesite is a rare component of this 'magmatic' ore mineral assemblage.

The small size of bowlesite (up to 20 µm across) prevented its crystallographic and structural characterisation. Therefore, its synthetic counterpart was synthesised and properly studied by X-ray diffraction. The identity between natural and synthetic samples was unequivocally confirmed by optical data, electron microprobe analyses and the structural identity by EBSD, and Raman spectroscopy.

References

Bachhuber F., Krach A., Furtner A., Söhnel T., Peter P., Rothballer J. and Weihrich R. (2015) Phase stabilities of pyrite-related MTCh compounds (M = Ni, Pd, Pt; T = Si, Ge, Sn, Pb; Ch = S, Se, Te): A systematic DFT study. Journal of Solid State Chemistry, 226, 29–35.

Ballhaus C.G. and Stumpfl E.F. (1986) Sulfide and platinum mineralization in the Merensky Reef: evidence from hydrous silicates and fluid inclusions. Contributions to Mineralogy and Petrology, 94, 193–204.

Bannister F.A. and Hey M.H. (1932) Determination of minerals in platinum concentrates from the Transvaal by X-ray methods. Mineralogical Magazine, 28, 188–206.

Barkov A.Y., Martin R.F., Kaukonen R.J. and Alapieti T.T. (2001) The occurrence of Pb–Cl–(OH) and Pt–Sn–S compounds in the Merensky reef, Bushveld layered complex, South Africa. The Canadian Mineralogist, 39, 1397–1403.

Barnes S.J. and Maier W.D. (2002) Platinum group elements and microstructures of normal Merensky Reef from Impala Platinum Mines, Bushveld Complex. Journal of Petrology, 43, 103–128.

Bayliss P. (1989) Crystal chemistry and crystallography of some minerals within the pyrite group. American Mineralogist, 74, 1168–1176.

Bruker AXS (2014) Topas 5, Computing Program. Bruker AXS GmbH, Karlsruhe, Germany.

Brynard H.J., de Villiers J.P.R. and Viljoen E.A. (1976) A mineralogical investigation of the Merensky Reef at the Western planium mine, near Marikana, South Africa. Economic Geology, 71, 1299–1307.

Cawthorn R.G. (2010) The platinum group element deposits of the Bushveld Complex in South Africa. Platinum Metals Review, 54, 205–215.

Cousins C.A. and Kinloch E.D. (1976) Some observations on textures and inclusions in alluvial platinoids. Economic Geology, 71, 1377–1398.

Groenvold F., Haraldsen H. and Kjekshus A. (1960) On the sulfides, selenides and tellurides of platinum. Acta Chemica Scandinavica, 14, 1879–1893

Kingston G.A. (1966) The occurrence of platinoid bismuthotellurides in the Merensky Reef at Rustenburg Platinum Mine in the Western Bushveld. Mineralogical Magazine, 35, 815–834

Kinloch E.D. (1982) Regional trends in the platinum-group mineralogy of the Critical Zone of the Bushveld Complex, South Africa. Economic Geology, 77, 1328–1347.

Kovalenker V.A., Begizov V.D., Evstigneeva T.L., Troneva N.V. and Ryabikin V.A. (1979) Maslovite, PtBiTe: a new mineral from the Oktyabr copper-nickel deposit. Geologia Rudnych Mestorozhdenii, 21, 94–104 [in Russian].

Mernagh T.P. and Trudu A.G. (1993) A laser Raman microprobe study of some geologically important sulphide minerals. Chemical Geology, 103, 113–127.

Mihálik P., Hiemstra S.A. and De Villiers I.P.R. (1975) Rustenburgite and atokite, two new platinum-group minerals from the Merensky Reef, Bushveld igneous complex. The Canadian Mineralogist, 13, 146–150.

Naldrett A.J. (2004) Magmatic Sulfide Deposits: Geology, Geochemistry and Exploration. Springer, Heidelberg, 727 pp.

Nicholson D.M. and Mathez E.A. (1991) Petrogenesis of the Merensky Reef in the Rustenburg section of the Bushveld Complex. Contributions to Mineralogy and Petrology, 107, 293–309.

Oberthür T., Weiser T.W., Gast L. and Kojonen K. (2003) Geochemistry and mineralogy of platinum-group elements at Hartley Platinum Mine, Zimbabwe. Mineralium Deposita, 38, 327–343.

Oberthür T., Melcher F., Gast L., Wöhrl C. and Lodziak J (2004) Detrital platinum-group minerals in rivers draining the Eastern Bushveld Complex, South Africa. The Canadian Mineralogist, 42, 563–582.

Oberthür T., Malte J., Rudashevsky N., de Meyer E. and Gutter P. (2016) Platinum-group minerals in the LG and MG chromitites of the eastern Bushveld Complex, South Africa. Mineralium Deposita, 51, 71–87.

Osbahr I. (2012) Platinum-group element distribution in base-metal sulfides of the Merensky Reef and UG2 from the eastern and western Bushveld Complex, South Africa. PhD thesis, Friedrich-Alexander Universität Erlangen-Nürnberg, GeoZentrum Nordbayern, Germany, pp 172.

Osbahr, I., Klemd, R., Oberthür, T., Brätz, H. and Schouwstra, R. (2013) Platinum-group element distribution in base-metal sulfides of the Merensky Reef from the eastern and western Bushveld Complex, South Africa. Mineralium Deposita, 48, 211–232.

Paar H.W., Topa D., Makovicky E. and Culetto F.J. (2005) Milotaite, (PdSbSe), a new palladium mineral species from Předbořice, Czech Republic. The Canadian Mineralogist, 43, 689–694.

Smith D.G.W. and Nickel E.H. (2007) A system for codification for unnamed minerals: report of the Subcommittee for Unnamed Minerals of the IMA Commission on New Minerals, Nomenclature and Classification. The Canadian Mineralogist, 45, 983–1055.

Vermaak C.F. and Hendriks L.P. (1976) A review of the mineralogy of the Merensky Reef, with special reference to new data on the precious metal mineralogy. *Economic Geology*, **71**, 1244–1269.

Vermaak C.F. and Von Gruenewaldt G. (1981) Third international platinum symposium, excursion guidebook. *Geological Society of South Africa and Society of Economic Geology*, 1–62, ISBN 0 7988 2117, 5.

Vymazalová A., Zaccarini F., Garuti G., Laufek F., Mauro D., Stanley C.J. and Biagioni C. (2019) Bowlesite, IMA 2019-079. CNMNC Newsletter No. 52; *Mineralogical Magazine*, 83, https://doi.org/10.1180/mgm.2019.73

Wagner P.A. (1929) *The Platinum Deposits and mines of South Africa*. Oliver and Boyd, Edinburgh, pp. 326.

Weihrich R., Kurowski D., Stückl A.C., Matar S.F., Rau F. and Bernert T. (2004) On the ordering in new low gap semiconductors: PtSnS, PtSnSe, PtSnTe. Experimental and DFT studies. *Journal of Solid State Chemistry*, **177**, 2591–2599.